

# PYROELECTRIC PROPERTIES OF La-Sr-Co-O/Pb-La-Ti-O/La-Sr-Co-O HETEROSTRUCTURES

August 1999

C. W. Tipton, R. C. Hoffman, and D. N. Robertson  
U.S. Army Research Laboratory  
Adelphi, Maryland 20783

R. P. Godfrey, T. Friessnegg, and R. Ramesh  
Department of Physics, University of Maryland  
College Park, Maryland 20742

M. A. Quijada  
Genesis Engineering,  
Lanham, Maryland 20706

## ABSTRACT

The realization of a commercially viable, *thin-film* uncooled pyroelectric detector has been the focus of research for several years. As part of this effort, we show that a conventional metallic electrode system (typically Pt) can be replaced with a conductive oxide such as  $\text{La}_x\text{Sr}_{(1-x)}\text{CoO}_3$  (LSCO). In addition to being crystallographically compatible with the lead-based, pyroelectric oxides such as  $\text{Pb}_{0.9}\text{La}_{0.1}\text{Ti}_{0.975}\text{O}_3$  (PLT10), LSCO is also chemically compatible, which aids in reducing the energy barrier for oriented growth and promotes the formation of phase-pure perovskite pyroelectric material. We have grown pyroelectric heterostructures of LSCO/PLT10/LSCO on single-crystal  $\text{LaAlO}_3$  substrates by pulsed laser deposition. By carefully optimizing the processing conditions, we are able to obtain high-quality, thin films that allow us to investigate the basic pyroelectric properties of this material system. Additionally, LSCO exhibits a strong infrared absorption ( $\alpha = 10^5/\text{cm}$ ), which is beneficial for producing a simplified detector design with enhanced performance. We will discuss the pyroelectric and dielectric properties of LSCO/PLT10/LSCO heterostructures and their dependence on microstructure. Structural characterizations reveal that the *c*-axis orientation of the PLT10 can be maximized. Pyroelectric measurements using the Byer-Roundy method have yielded, on the average, pyroelectric coefficients of  $50 \text{ nC/cm}^2\text{K}$  for PLT10. Both pyroelectric coefficients and pulsed polarization values show a clear dependence on the *c*-axis volume fraction of the PLT10 films. Finally, the Byer-Roundy technique is being used to study the impact of electronic defects on the pyroelectric response of these heterostructures.

## 1.0 INTRODUCTION

Recent research has focused on the realization of a commercially viable, thin-film uncooled pyroelectric detector. Since the pyroelectric response is directly related to the orientation of the spontaneous polarization, a fundamental understanding of several important materials issues is needed. These include the role of crystallographic orientation, polarization domain structure, electronic defect concentration, and the significance of the role of defect dipoles. For example, a random orientation of the polarization direction (as in the case of a polycrystalline material) leads to a small pyroelectric response, especially under unpoled conditions. Furthermore, polarization relaxation in

## Form SF298 Citation Data

<b>Report Date</b> <i>("DD MON YYYY")</i> 00081999	<b>Report Type</b> N/A	<b>Dates Covered (from... to)</b> <i>("DD MON YYYY")</i>
<b>Title and Subtitle</b> Pyroelectric Properties of La-Sr-Co-O/Pb-La-Ti-O/La-Sr-Co-O Heterostructures		<b>Contract or Grant Number</b>
<b>Authors</b>		<b>Program Element Number</b>
<b>Performing Organization Name(s) and Address(es)</b> U.S. Army Research Laboratory Adelphi, Maryland 20783		<b>Project Number</b>
<b>Sponsoring/Monitoring Agency Name(s) and Address(es)</b>		<b>Task Number</b>
<b>Distribution/Availability Statement</b> Approved for public release, distribution unlimited		<b>Work Unit Number</b>
<b>Supplementary Notes</b>		<b>Performing Organization Number(s)</b>
<b>Abstract</b>		<b>Monitoring Agency Acronym</b>
<b>Subject Terms</b>		<b>Monitoring Agency Report Number(s)</b>
<b>Document Classification</b> unclassified	<b>Classification of SF298</b> unclassified	
<b>Classification of Abstract</b> unclassified	<b>Limitation of Abstract</b> unlimited	
<b>Number of Pages</b> 10		

these materials will play a role in the time dependence of the pyroelectric response. It is expected that both 90 degree and 180 degree domains (the two types of domains present in tetragonal perovskite materials) will play a dominant role in the observed magnitude of the pyroelectric response. Also, the influence of electronic defects may suppress or enhance the pyroelectric response. In this paper, we focus on a prototypical heterostructure within which the domain structure and defect chemistry can be systematically controlled to study their influence on this heterostructure's pyroelectric properties.

## 2.0 EXPERIMENTAL METHOD

Thin-film heterostructures were fabricated on (001) single-crystal  $\text{LaAlO}_3$  (LAO) substrates using a pulsed KrF (248 nm) excimer laser deposition (PLD) system to ablate ceramic targets of  $\text{La}_{(1-x)}\text{Sr}_x\text{CoO}_3$  (LSCO) and  $\text{Pb}_{0.9}\text{La}_{0.1}\text{Ti}_{0.975}\text{O}_3$  (PLT10). Figure 1 shows the idealized cross-section of the pyroelectric capacitor studied in this work. Individual capacitors in this structure were defined by standard photolithographic lift-off and wet-etching techniques. The bottom LSCO electrode is common to all capacitors on the substrate. Nominal film thickness was 80 nm for both top and bottom LSCO electrodes and 200 nm for the PLT10 layer. Depositions were performed in an  $\text{O}_2$  environment at pressures between 10 and 100 mTorr. The substrate heater temperature during deposition was varied between 500 and 700 °C to vary the degree of *c*-axis orientation of the PLT10 layer. Pt contacts with a Ti adhesion layer were deposited via sputtering for electrical contacts.

Structural characterizations were performed with a four-circle Siemens D5000 diffractometer using a copper  $\text{K}_\alpha$  radiation source. Ferroelectric measurements were taken with a Radiant Technologies RT66A testing station and dielectric measurements were made with a Hewlett-Packard 4192A impedance analyzer. Pyroelectric measurements were made using a computer-controlled system based on a Keithley 6517A electrometer and a Temptronic heat/cool chuck.

### 2.1 OXIDE ELECTRODES

Earlier work<sup>[1,2,3,4]</sup> has shown that highly oriented and in some cases epitaxial ferroelectric layers can be grown on suitable surfaces, for example, single-crystalline oxide substrates. Heteroepitaxy in ferroelectric PLT10 layers has been promoted through the use of a lattice and chemically matched bottom electrode material—the perovskite structured LSCO<sup>[5]</sup>. The bottom LSCO electrode stabilizes the growth of pyrochlore-free PLT10 throughout a larger temperature range (500 to 700 °C) than is possible with nonoxide-based electrodes.

The conducting properties of LSCO thin films have been previously reported<sup>[6]</sup>. In addition to being crystallographically compatible with the lead-based pyroelectric oxides such as PLT10, LSCO also has excellent infrared absorption properties. Figure 2 gives the absorption coefficient,  $\alpha$ , of bulk  $\text{La}_{0.5}\text{Sr}_{0.5}\text{CoO}_3$ . The infrared absorption is approximately  $1 \times 10^5 \text{ cm}^{-1}$  over the relevant IR wavelengths of 8 to 14  $\mu\text{m}$ . The absorption characteristics of LSCO help to simplify pyroelectric detector design via the use of a single LSCO layer for both electrode and absorbing layer. The ability to adjust the transmission and absorption properties of the detector structure, especially those structures incorporating a resonant cavity<sup>[7]</sup>, is very important for maximizing the pyroelectric response.

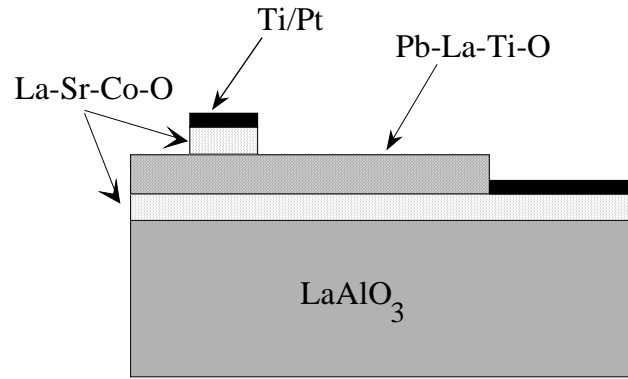


Figure 1. Pyroelectric heterostructure.

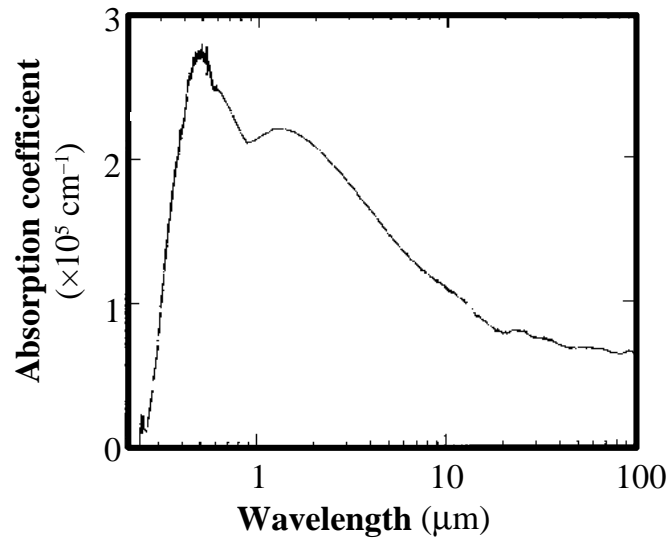


Figure 2. Infrared absorption spectrum of bulk  $\text{La}_{0.5}\text{Sr}_{0.5}\text{CoO}_3$ .

### 3.0 RESULTS AND DISCUSSION

Figure 3 gives the x-ray diffraction spectra of four heterostructures deposited at substrate heater temperatures of 500, 550, 600, and 650 °C. A qualitative analysis of this figure shows that as the growth temperature is increased, the volume fraction of *c*-axis-oriented perovskite material also increases. At a deposition temperature of 600 °C, the PLT10 layer is a mixture of *c*-axis-oriented and *a*-axis-oriented material. While at 650 °C, it is almost fully *c*-axis-oriented. Thus, by controlling the deposition temperature, we can directly control crystallographic orientation within the PLT10 layer. There are additional effects that influence *c*-axis orientation that must be considered, such as composition, strain, and film thickness. We have attempted to minimize the variations in these parameters carefully controlling all processing parameters.

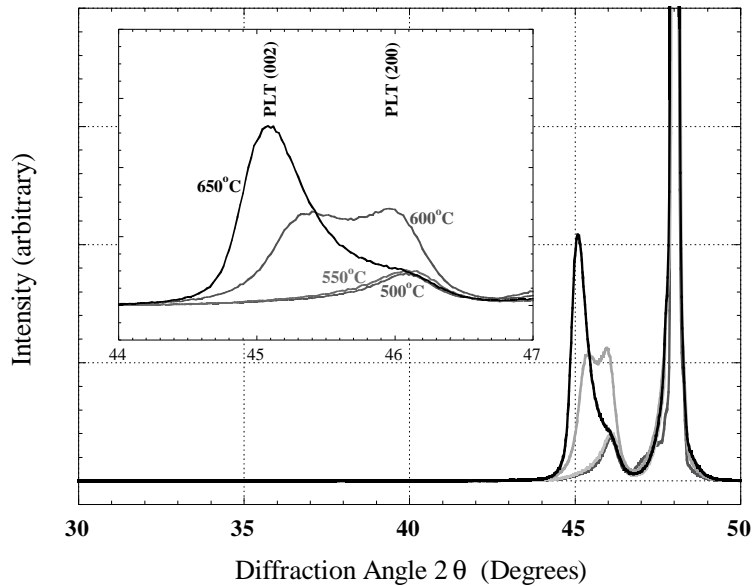


Figure 3. X-ray diffraction spectra for LSCO/PLT10/LSCO films deposited at different substrate temperatures. Inset shows enlarged spectra for *a*-axis and *c*-axis PLT10 peaks.

### 3.1 POSITRON ANNIHILATION

A variety of approaches to studying material defects exist. Positron annihilation spectroscopy (PAS) probes the defect structure by implanting positrons and analyzing the spectrum of emitted photons resulting from positron-electron annihilations that occur within the material of interest. The spectrum is characterized by the *S*-parameter value, which gives a relative value for the defect concentrations. Larger *S*-parameter values correspond to higher vacancy concentrations. Further details on the PAS technique are well documented elsewhere<sup>[8, 9, 10]</sup>.

The defect structure of our films has been studied using PAS with a variable-energy positron beam. The *S*-parameter as a function of positron energy is shown in figure 4. The variation in positron energy probes different

depths of the film such that the energy axis may be taken as being equivalent to penetration depth with an additional calibration factor. The large peak in the  $S$ -parameter over the energy range of 5 to 12 keV corresponds to the PLT10 layer in the heterostructure. Samples grown at 650 and 700 °C, both of which exhibited largely  $c$ -axis orientation, show significantly lower  $S$ -parameters for the PLT10 layer. This corresponds to a dramatically lower defect concentration and/or defect size relative to the samples grown at lower temperatures, which exhibit mostly  $a$ -axis orientation.

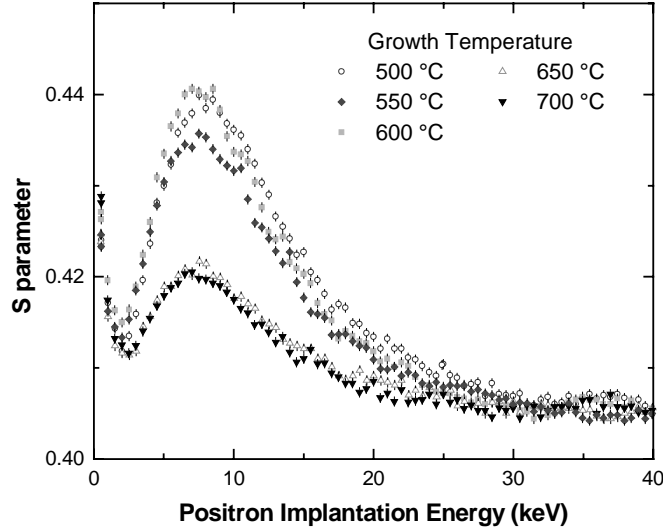


Figure 4. Positron annihilation spectroscopy results for PLT10 films with LSCO electrodes grown at different deposition temperatures.

### 3.2 FERROELECTRIC AND PYROELECTRIC PROPERTIES

Polarization hysteresis loops shown in figure 5 were taken on the same series of samples used in figure 3. The saturation and remnant polarization values show a systematic increase with increasing deposition temperature.

The pyroelectric response was measured using the Byer-Roundy method<sup>[11]</sup>. The pyroelectric coefficient can be calculated by

$$p(T) = I_p(T) \left[ A \frac{dT}{dt} \right]^{-1} \quad (1)$$

where  $I_p(T)$  is the measured pyroelectric current as a function of temperature,  $A$  is the capacitor area, and  $dT/dt$  is the temperature ramp applied to the capacitor. Figure 6 shows the measured pyroelectric response of a  $2.5 \times 10^{-5} \text{ cm}^2$  capacitor grown at 600 °C. Consistent with equation (1), the pyroelectric response is essentially proportional to the time derivative of the temperature ramp. The change in current of 1.4 pA at 25 °C corresponds to a pyroelectric coefficient of 45 nC/cm<sup>2</sup> K.

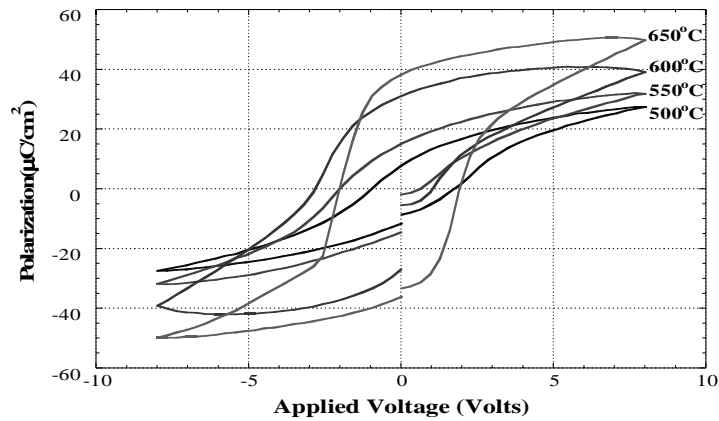


Figure 5. Polarization hysteresis loops of  $2.5 \times 10^{-5} \text{ cm}^2$  capacitors grown at different deposition temperatures.

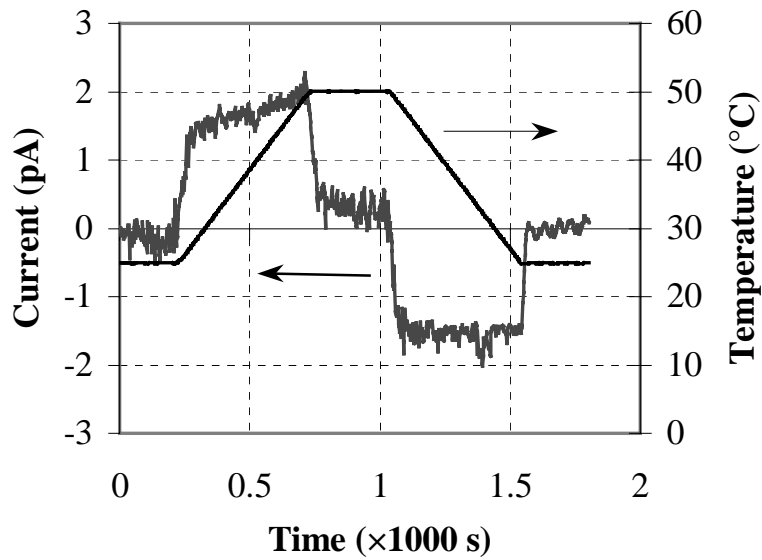


Figure 6. Pyroelectric current for a  $2.5 \times 10^{-5} \text{ cm}^2$  capacitor with an applied temperature ramp rate of  $3 \text{ }^\circ\text{C}/\text{min}$ . The temperature profile is plotted against the right-hand vertical axis.

A slight time dependence in the pyroelectric current is observed as the temperature ramps from 25 to  $50 \text{ }^\circ\text{C}$ . This is an obvious deviation from the ideal response, which would produce a constant current during the linear temperature ramp. This time-dependent characteristic has been observed in many samples, including those

produced by deposition methods other than PLD and those using Pt electrodes instead of LSCO. Based on our initial experiments, we attribute this nonideal response to the presence of "dipoles", such as those found in heteropolar electrets<sup>[12]</sup>, that have shortened thermal lifetimes at elevated temperatures. We have observed that upon annealing at temperatures higher than the maximum ramped temperature, this time-dependent characteristic is eliminated. We suggest that annealing allows these dipoles to thermally relax, thus giving a near-ideal pyroelectric response.

At this point it is appropriate to comment on the techniques used to measure the pyroelectric coefficient. In a recent article, Daghli<sup>[13]</sup> reviewed the several methods used by researchers to determine the pyroelectric coefficient. He points out that the polarization-electric field (P-E) technique is rarely used due to its limited accuracy. After reviewing recent articles in which the P-E technique was used, we take a stronger position and recommend that this technique *not* be used. Certainly, one could argue that this method lacks the resolution or that polarization stabilization is not achieved or that temperature-dependant leakage currents may overwhelm the pyroelectric response. Additionally, this technique only measures those dipoles that are electrically switchable! If through defects and/or grain boundaries a majority of domains are pinned in one direction of the polar axis, the P-E measurement would underestimate the true pyroelectric response. Figures 7 and 8 give the pyroelectric response of a PLT10 capacitor. Figure 7 shows the P-E measurements from 25 to 125 °C used to obtain this pyroelectric coefficient. Figure 8 compares the pyroelectric coefficients obtained through the P-E and Byer-Roundy techniques. Since these measurements are made far from the Curie temperature, one expects that the pyroelectric coefficient to be nearly constant as seen in the Byer-Roundy data. Although the quasi-static Byer-Roundy method may not give the true pulsed-temperature response it is certainly more accurate than the P-E technique.

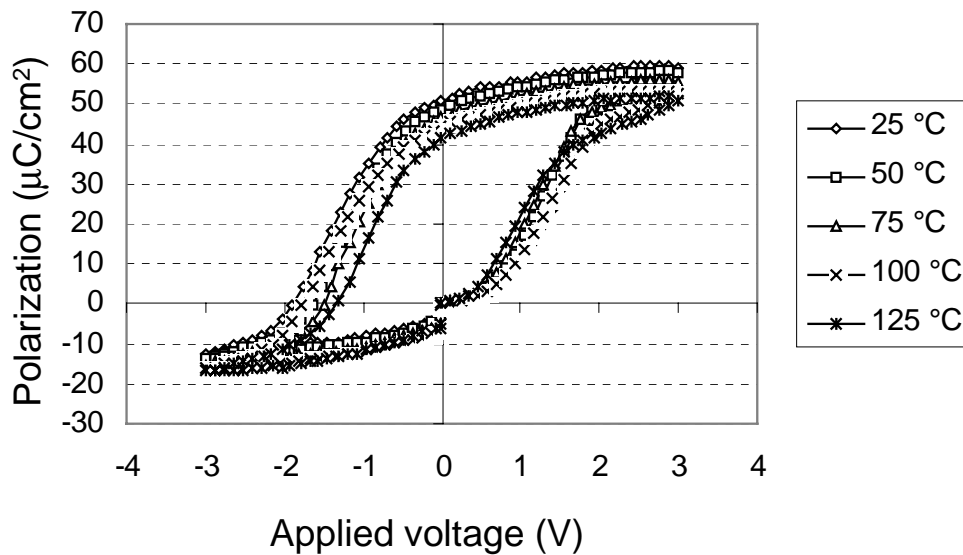


Figure 7. Ferroelectric hysteresis loops of a PLT10 capacitor as a function of temperature.

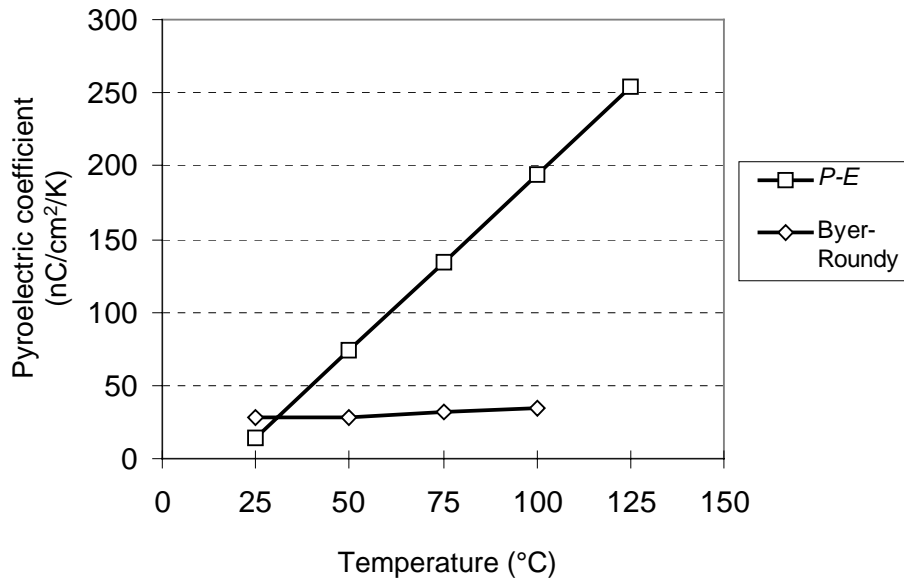


Figure 8. Pyroelectric coefficients of a  $1 \times 10^{-4} \text{ cm}^2$ , PLT10 capacitor as determined by the Byer-Roundy and  $P$ - $E$  hysteresis loop techniques.

The results of our pyroelectric and dissipation factor measurements are summarized in figure 9. The dissipation factor was assessed at a frequency of 1 kHz and a signal amplitude of 100 mV. We speculate that the loss of Pb at high processing temperatures has produced a significant number of vacancies, thereby allowing greater domain motion and/or defect-related dipoles and, hence, greater dielectric loss.

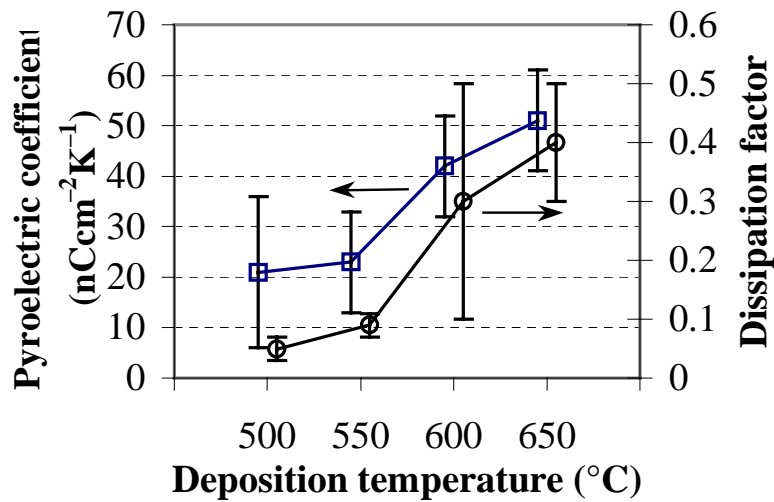


Figure 9. Pyroelectric coefficient and dissipation factor of PLT10 heterostructures as function of deposition temperature. All data obtained after device poling.

### 3.3 POLING EFFECTS

Two samples used in this study were electrically poled to ascertain the effect of 90 degree domains on the pyroelectric response. Figure 10 shows the results for samples deposited at 650 and 500 °C (*c*-axis- and *a*-axis-oriented, respectively). Both samples were initially poled at -2 V (dc) at 150 °C. Additional room-temperature pyroelectric measurements were taken after poling the sample with a single, 1-ms square pulse at several voltages up to 4 V. In this figure, one can see that electrical poling, as expected, has a more significant affect in 180 degree domain material.

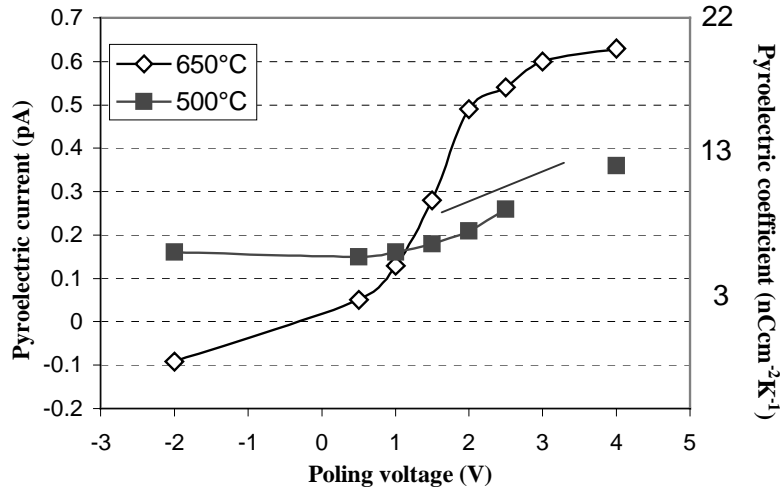


Figure 10. Room temperature pyroelectric response as a function of pulsed (1 ms) poling voltage. Samples were initially poled at -2 V and 150 °C.

### 4.0 SUMMARY

In summary, we have demonstrated the use of LSCO electrodes for pyroelectric devices. LSCO electrodes are beneficial for stabilized PLT10 growth and they have excellent infrared absorption properties. Our thin-film heterostructures have, on average, a pyroelectric coefficient of approximately 50 nC/cm<sup>2</sup>K, which is comparable to data previously published for much thicker films. We are continuing our investigation of the impact of electronic defects on the pyroelectric response of thin films.

### 5.0 ACKNOWLEDGMENTS

Support for this work came from the U.S. Army Research Laboratory through the Microelectronics Research Collaborative Partnership.

---

## 6.0 REFERENCES

- [1] S. Stemmer, et al., *J. Mater. Res.* **10**, 791 (1995).
- [2] W. Ma, et al., *Ferroelectric Lett.* **23**, 153 (1998).
- [3] H. Tabata, et al., *Appl. Phys. Lett.* **64**, 428 (1994).
- [4] R. Takayama, et al., *Ferroelectrics* **118**, 325 (1991).
- [5] R. Ramesh, et al., *Appl. Phys. Lett.* **64**, 2511 (1994).
- [6] S. Madhukar, et al., *J. Appl. Phys.*, **81**, 3543 (1997).
- [7] W. A. Beck, et al., "Infrared absorption by ferroelectric thin-film structures," *Proc. 1998 IRIS Specialty Group on Infrared Mater.*, (1998).
- [8] D. J. Keeble et al. *Appl. Phys. Lett.* **73**, 508 (1998).
- [9] D. J. Keeble et al. *Appl. Phys. Lett.* **73**, 318 (1998).
- [10] Positron Spectroscopy of Solids, Proceedings of the International School of Physics "Enrico Fermi," Varena, Italy, A. Dupasquier and A.P. Mills Jr., eds., IOS Press Ohmsha, (1993).
- [11] L. Byer and C. B. Roundy, *Ferroelectrics* **3**, 333 (1972).
- [12] M. E. Lines and A. M. Glass, *Principles and Applications of Ferroelectrics and Related Materials*, Oxford University Press (1996), pp. 547-550.
- [13] M. Daglish, *Integrated Ferroelectrics* **22**, 473 (1998).